

Vision-aided Dynamic Quadrupedal Locomotion on Discrete Terrain using Motion Libraries

Ayush Agrawal^{1,2}, Shuxiao Chen¹, Akshara Rai² and Koushil Sreenath¹

Abstract—In this paper, we present a framework rooted in control and planning that enables quadrupedal robots to traverse challenging terrains with discrete footholds using visual feedback. Navigating discrete terrain is challenging for quadrupeds because the motion of the robot can be aperiodic, highly dynamic, and blind for the hind legs of the robot. Additionally, the robot needs to reason over both the feasible footholds as well as robot velocity by speeding up and slowing down at different parts of the terrain. We build an offline library of periodic gaits which span two trotting steps on the robot, and switch between different motion primitives to achieve aperiodic motions of different step lengths on an A1 robot. The motion library is used to provide targets to a geometric model predictive controller which controls stance. To incorporate visual feedback, we use terrain mapping tools to build a local height map of the terrain around the robot using RGB and depth cameras, and extract feasible foothold locations around both the front and hind legs of the robot. Our experiments show a Unitree A1 robot navigating multiple unknown, challenging and discrete terrains in the real world.

I. INTRODUCTION

Legged robots have the unique capability to traverse across a wide variety of challenging and rough terrain, including terrains with gaps and discrete footholds. To navigate such terrain, a legged robot needs to precisely place its feet on feasible footholds, while maintaining its overall stability. This requires planning over multiple footsteps, as well as desired robot motion between the footsteps. For example, the robot might need to slow down, and take a few steps on the same foothold, before speeding up and stepping over a large gap. Moreover, for unknown discrete terrain, the robot needs to make these decisions in real-time while navigating; stopping might make the robot unstable and gaps harder to cross. This results in a high-dimensional and complex optimization problem with a limited compute time budget.

One promising approach for solving footstep selection problems in literature is by building a library of two-step periodic gaits for bipedal robots [1], [2], [3]. However, two-step periodic gaits are overly restrictive for quadrupedal robots since it enforces a symmetry constraint between consecutive steps on the robot. On uneven, discrete terrain,



Fig. 1: A1 robot walking over a random discrete terrain using our proposed approach. Video of experiments can be found here: <https://youtu.be/3HAUvSsQYjs>.

the robot might not be able to reach the same initial state within two steps, and might need multiple steps to reach it.

In this work, we create an offline motion library of two-step periodic trotting gaits for a quadrupedal A1 robot, which consist of four stance phases (equivalent to four bipedal steps).

By switching between different motion primitives, we can effectively achieve aperiodic locomotion on a quadruped.

Discrete, uneven terrains present an additional challenge of controlling the robot in different orientations. Popular model-based quadrupedal control techniques like [4] assume linearized models of the robot about zero roll, pitch, yaw of the torso. Such models are not suitable for uneven terrains which can result in the robot pitching, or experiencing high angular velocities. We present a coordinate-free linear dynamics model that uses rotation matrices, instead of Euler orientations, building on recent works on variational-based linearization. Next, we formulate a Quadratic Program (QP) that uses this dynamics model and outputs torques that can achieve desired footstep and center of mass (CoM) velocity targets output by the motion library. This CoM model adds stability and robustness to our controller, and enables our robot to navigate long, challenging terrains reliably. In comparison, a controller using a linearized CoM dynamics model suffers and experiences frequent falls on the robot.

A. Related Work

Legged locomotion on discrete terrain, such as across stepping stones, is an active area of research with methods ranging from reduced-order models, to learning-based approaches. We surmise different directions here:

Reduced Order Models: In [5], authors propose a reduced

This work is supported in part by Facebook AI Research through BAIR Open Research Commons and in part by National Science Foundation Grant CMMI-1944722.

¹Authors are with the Department of Mechanical Engineering, University of California, Berkeley {ayush.agrawal, shuxiao.chen, koushils}@berkeley.edu

²Authors are with Facebook AI Research, {agrawalayush, akshararai}@fb.com

order cart-pole model to generate gaits for a bipedal robot to walk on randomly placed stepping stones. [6] presents a method to regulate the center-of-pressure to guide the robot leg onto a discrete foothold. More recently, in [7], a reduced-order linear inverted pendulum model is presented to regulate the angular momentum about the stance foot at discrete impacts through the vertical center of mass velocity. A QP-based controller is then used to track outputs for 2D bipedal robots to walk on discrete terrain.

Trajectory Optimization and Optimal Control: Optimization-based controllers such as Control Barrier Functions (CBFs) and Model Predictive Control (MPC) can enforce state and input constraints. In [8], [9], a CBF-based approach regulates the foot positions of a bipedal robot around a nominal periodic gait, to step on discrete footholds. This method is extended in [10] to use a library of walking gaits. The work in [1], [2], [3] leverages the use of two-step periodic gaits, computed offline through trajectory optimization, to transition between gaits of different step lengths online. In [11], a multi-layered optimal control framework is presented that combines CBFs with MPC for precise foot placement over a planning horizon.

Reinforcement Learning (RL): [12] learn a high-level footstep planner, that takes in the local height-map of the terrain as input, and outputs a sequence of desired footstep locations. A low-level joint controller is then learned to track these footsteps. In [13], the authors propose learning the desired accelerations for a centroidal model of a quadruped and use a heuristic approach to plan for footsteps on discrete terrain. The work in [14] proposes a curriculum with varying levels of difficulty to learn a policy for various bipedal robots to walk across stepping-stones. Several methods such as in [15] and [16] have also explored combining learning based approaches, particularly for vision-based footstep planning along with model-based low-level joint control.

B. Approach and Primary Contributions

In this work, we study the problem of dynamic locomotion for quadrupedal robots across discrete terrain, with visual feedback. We extend our prior work [2], [1], [3] on using motion libraries for bipedal locomotion to quadrupedal locomotion over discrete terrain. Our method leverages offline computation of a motion library for trotting gaits at different step lengths, achieving aperiodic gaits by switching between motion primitives. We use a geometric MPC approach to translate optimized targets to joint torques on the A1 robot. Additionally, using the mapping framework developed in [17], [18], we use a depth camera to build a local map of the terrain around the robot. We experimentally validate our proposed approach on the Unitree A1 quadrupedal robot and show the robot navigating multiple unknown, challenging discrete terrains.

II. HYBRID MODEL OF TROTTING

In this section, we introduce the necessary background and notations for the robot dynamics model considered in

our approach. Our formulation of the dynamics is derived from prior work on hybrid dynamics, like [2].

Configuration Variables: The Unitree A1 is a four legged robot with 3 motors in each leg, weighing around 10kg with 12 actuated degrees of freedom and 6 underactuated base degrees of freedom. The configuration of the robot is represented by the vector $q = [p, \Theta, q_{FR}, q_{FL}, q_{RR}, q_{RL}] \in \mathcal{Q} \subset \mathbb{R}^{18}$, where $p \in \mathbb{R}^3$ denotes the Cartesian position of the robot in the world frame, $\Theta \in \mathbb{R}^3$ denotes the ZYX Euler angle representation of the orientation of the body, and $q_i \in \mathbb{R}^3$, $i \in \{FR, FL, RR, RL\}$ denotes the actuated joints of the front/rear right/left legs. The actuated joints include hip abduction, hip pitch and knee pitch degrees of freedom.

Continuous Dynamics: The dynamics model of each of phase of a trotting gait can be obtained through the method of Lagrange and represented by the *Manipulator equations*:

$$D(q)\ddot{q} + C(q, \dot{q})\dot{q} + G(q) = B\tau + J_c^T \lambda_c, \quad (1)$$

$$J_c \ddot{q} + \dot{J}_c \dot{q} \equiv 0, \quad (2)$$

where D is the inertia matrix, C the Coriolis terms, G gravitational terms, B a selection matrix. J_c denotes the contact Jacobian, λ_c denotes the contact forces at the feet, and $\tau \in \mathbb{R}^{12}$ denotes the motor torques. The dimension of J_c and λ_c depend on the phase of gait, and number of legs in contact with the ground.

Impact Dynamics: The collision of the feet with the ground is modelled as an instantaneous rigid impact and the post-impact velocities \dot{q}^+ can be obtained by solving the linear system of equations:

$$\begin{bmatrix} D(q) & -J_c^T(q) \\ J_c(q) & 0 \end{bmatrix} \cdot \begin{bmatrix} \dot{q}^+ \\ \lambda_c \end{bmatrix} = \begin{bmatrix} D(q)\dot{q}^- \\ 0 \end{bmatrix}. \quad (3)$$

Hybrid Model: Combining (1) and (3), we obtain a hybrid dynamical model for trotting as,

$$\begin{aligned} \Sigma_{ds} : \begin{cases} \dot{x} &= f_{ds}(x) + g_{ds}(x)\tau, \quad (x, \tau) \notin \mathcal{S}_{ds \rightarrow qs} \\ x^+ &= \Delta_{ds \rightarrow qs}(x^-), \quad (x, \tau) \in \mathcal{S}_{ds \rightarrow qs} \end{cases} \\ \Sigma_{qs} : \begin{cases} \dot{x} &= f_{qs}(x) + g_{qs}(x)\tau, \quad x \notin \mathcal{S}_{qs \rightarrow ds} \\ x^+ &= \Delta_{qs \rightarrow ds}(x^-), \quad x \in \mathcal{S}_{qs \rightarrow ds} \end{cases}, \end{aligned} \quad (4)$$

where $x := [q, \dot{q}]'$ is the state of the robot, $\mathcal{S}_{ds \rightarrow qs} := \{(x, \tau) \mid \lambda_c^z(x, \tau) = 0\}$ is the switching surface corresponding to the transition between double support and quadruple support domains and is defined as the set of states and control inputs such that the vertical ground reaction force $\lambda_c^z(x, \tau) \equiv 0$ (this corresponds to the case when the stance foot lifts off from the ground). The switching surface $\mathcal{S}_{qs \rightarrow ds} := \{x \mid p_{sw}^z(x) = 0\}$ corresponding to the transition between flight to stance as the set of states such that the vertical component of the position of the swing foot is zero.

In addition, $\Delta_{qs \rightarrow ds} = \mathbb{I}$ is the identity operator and $\Delta_{ds \rightarrow qs}$ is obtained from rigid impact dynamics. $f_{ds}(x)$, $g_{ds}(x)$ and $f_{qs}(x)$, $g_{qs}(x)$ denote the vector-fields in the double-support and quadruple-support phases respectively,

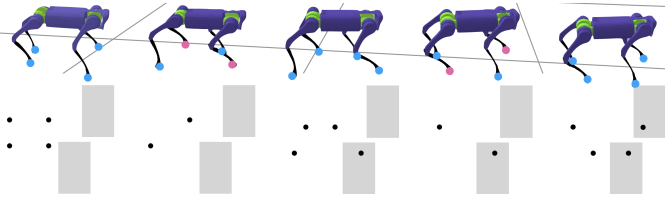


Fig. 2: A trotting step on the A1 quadruped consists of two ‘single’ stance phases where the diagonal legs are in contact, and two ‘double’ stance phases where all four legs are in contact. When walking over discrete terrain, one-step periodic gaits (comprised of two ‘single’ stance and two ‘double’ stance phases) can be overly restrictive. A two-step periodic gait (four ‘single’ stance and four ‘double’ stance phases) provides sufficient flexibility.

and are obtained using Lagrange’s equations of motion (1). Each trotting step comprises of two alternating phases of double and quadruple support as illustrated in Fig. 2.

III. TRAJECTORY OPTIMIZATION FOR TROTTING GAITS

We now present our proposed approach of trajectory optimization and low-level robot control using geometric model predictive control. We build a gait library consisting of gaits parametrized by step length and optimized to minimize the total torque over a trajectory given dynamics and periodicity constraints. Next, we present a model-based low-level controller that takes optimized CoM velocities and footstep locations from the gait library to generate desired joint torques that are applied on the robot. Lastly, we describe the localization and mapping framework we use for terrain mapping in real-world experiments.

A. Trajectory Optimization

In this section, we present a method to generate a motion library of trotting gaits that achieve foot-placements of different step lengths. We define each trotting step to comprise of In particular, we obtain gaits that are two-step-periodic, such that the post-impact states of the robot after two trotting steps return to the initial states at the start of the first step. The gaits are parametrized by the step-lengths in the first and second trotting step l_0 and l_1 respectively. For a trotting gait, the step lengths l_0 and l_1 each represent a pair of distances between the front stance and front swing feet and the hind stance and swing feet. The goal of trajectory optimization is then to find gait parameters $\gamma(l_0, l_1)$ for various step-length pairs to construct a library of gaits denoted by

$$\mathcal{G} := \{\gamma(l_0, l_1) \mid (l_0, l_1) \in \mathbb{L} \times \mathbb{L}\}, \quad (5)$$

where $\mathbb{L} := L \times L$ is a predefined set of step length pairs. Specifically, we choose $L = \{-0.2, -0.1, 0.0, 0.1, 0.2\}$ m, with a total of 625 gaits in the gait library. Specifically, $\gamma(l_0, l_1)$ comprises of the trajectory parameters of the average base linear velocities, height, body orientation and angular velocity, which are required by the MPC controller as described in Section III-C.

The trajectory optimization problem to obtain the gait library is solved using Direct Collocation which involves

discretizing each phase in time by a specified number of nodes N [19], with the objective of minimizing energy over the entire trajectory, subject to dynamics and additional constraints $c_i(x_i(t), \tau_i(t))$,

$$\begin{aligned} (x^*(\cdot), \tau^*(\cdot)) &= \arg \min_{x(t), \tau(t)} \sum_i \int_0^T \|\tau(t)\|_2^2 dt \\ \text{st. } x(t) &= \int_0^T f_i(x(t)) + g_i(x(t))\tau(t)dt, \\ c_i(x(t), \tau(t)) &\leq 0, \quad 0 \leq t \leq T, \quad \forall i \in \mathcal{I}. \end{aligned} \quad (6)$$

Here, the set \mathcal{I} denotes the set of all discrete phases, $c_i(x(t), \tau(t))$ encodes physical constraints such as state and input limits, friction constraints as well as *periodicity constraints* and step length constraints. The desired gait parameters $\gamma(l_0, l_1)$ can then be extracted from the optimal state trajectories $x^*(\cdot)$. We use the open-source optimization and simulation toolbox C-FROST [20] to perform the above optimization. We refer the reader to [2] for more details on the specifics of the trajectory optimization scheme.

Remark 1: The generation of two-step periodic gaits poses additional challenges and constraints compared to the two-step periodic gaits for bipedal robots in [2]. These challenges arise from kinematic constraints imposed between the front and the hind limbs. In particular, to independently choose the step length pairs l_0 and l_1 , and also induce periodicity constraints, we define each trotting step to be composed of two stance phases (one where the front-left and hind-right legs are in stance and the other where the front-right and hind-left are in stance), as opposed to a single stance phase. The two trotting steps then comprise of four stance phases, with the additional constraint that the net displacement of each the left and right sides must be equal.

B. Footstep Planning and Gait Selection

Once we have created the gait library, we can extract desired gait variables by querying motions that satisfy the environment foothold constraints and start from the current state of the robot.

Footstep Planning: To chose a desired foothold location, we first query the gait library to obtain a nominal foothold location based on the current configuration and center-of-mass velocity of the robot as well as a nominal desired center-of-mass velocity. Similar to [13], we then chose a desired step-length that is closest to the nominal foothold location and on the feasible terrain.

Gait Selection: Given the current state of the robot and the feasible footstep map, we extract a gait from the library based on the current step-length l_0 and the desired step-length l_1 through bi-linear interpolation of the gait library [2]. This returns the desired states for a reduced-order rigid-body model considered in the MPC controller. This update allows us to re-target the desired center-of-mass velocities to be consistent with the desired step-lengths.

C. Geometric Model Predictive Control for Stance

We now present our Geometric Model Predictive Control (MPC) framework, which outputs the joint torques of the stance legs with the objective to stabilize the robot's center-of-mass trajectory and body orientation. MPC is a widely used method for control of quadrupedal robots, but requires a linearization of CoM dynamics to simplify the underlying optimization for efficient real-time computations. A common approach to linearizing the CoM dynamics involves small angle approximation of the body roll and pitch and a *Jacobian* linearization of the orientation dynamics [4]. However, the small-angle approximation, restricts the domains in which the model is valid, especially on uneven terrain where the robot might experience high angular velocities and pitch due to disturbances. Additionally, since the dynamics of the robot body evolve on an $SE(3)$ manifold, singularity issues arise in the Jacobian linearization process. Euler discretization of the continuous-time orientation dynamics also results in the loss of the underlying geometric structure of the $SO(3)$ manifold and, as a result, the discrete-time dynamics are not energy preserving. This has led to research in geometric variational-based optimal control approaches [21], [22], [23] that linearize the quadruped dynamics using *rotation matrices* instead of Euler angles. The resulting linearization is coordinate free, holds in all orientations (not just close to 0 roll, pitch), and does not suffer from singularities. However, [21] do not consider discrete time dynamics of the linearized system required for MPC, and [23] use forward Euler to discretize the orientation dynamics. Euler discretization for orientations that lie on $SO(3)$ does not preserve energy, and the predicted future angular velocities do not lie in the tangent space of $SO(3)$.

We present Geometric variational MPC (GVMP) which applies a variational-based linearization [22] to a reduced-order model of the quadruped, while ensuring that the discretized system is energy conserving. Similar to prior works, we model the quadruped as a single rigid body actuated by linear forces and moment about its CoM.

Consider the system Lagrangian discretized using the Trapezoidal rule [24] with a time step of $\Delta t := t_{k+1} - t_k$:

$$\mathcal{L}_k \approx \int_{t_k}^{t_{k+1}} \mathcal{L} dt = \mathcal{L} \Delta t, \quad (7)$$

where \mathcal{L} is the Lagrangian in continuous-time.

To obtain the discrete-time dynamics of the system, we equate the action-sum to zero,

$$\sum_{k=0}^{N-1} \delta \mathcal{L}_k + \delta \mathcal{W}_k = 0, \quad (8)$$

where $\delta \mathcal{W}_k$ is the infinitesimal work done by the linear force f_k and moment τ_k ,

$$\delta \mathcal{W}_k := \Delta t (f_k \cdot \delta p_k + \tau_k \cdot \delta \eta_k), \quad (9)$$

where δp_k is an infinitesimal displacement and $\delta \eta_k \in \mathbb{R}^3$ can be thought of as an infinitesimal change in orientation.

The discrete-time equations of motion for the rigid-body dynamics is then,

$$p_{k+1} = p_k + \dot{p}_k \Delta t, \quad (10)$$

$$\dot{p}_{k+1} = \dot{p}_k + \Delta t \mathbf{g} + \frac{f_{k+1}}{m} \Delta t, \quad (11)$$

$$R_{k+1} = R_k \Delta R_k, \quad (12)$$

$$I \omega_{k+1} = \Delta R_k^T I \omega_k + \Delta t \tau_{k+1}, \quad (13)$$

where $R_k \in SO(3)$ denotes the rotation matrix, $I \in \mathbb{R}^{3 \times 3}$ is the inertia tensor, $\mathbf{g} \in \mathbb{R}^3$ is the gravity vector. $\Delta R_k := \exp(\Delta t \hat{\omega}_k)$ denotes the change in orientation of the body from time t_k to time t_{k+1} , where the exponential map $\exp : \mathfrak{so}(3) \rightarrow SO(3)$ maps a skew-symmetric matrix to a rotation matrix. We define the state of the rigid body to be $\xi_k := [p_k, \dot{p}_k, R_k, \omega_k]^T$ and the input to be $F_k := [f_k, \tau_k]^T$.

Remark 2: Equation (9) represents the discrete-time version of the principle of least-action, and any trajectory-input pair (ξ_k, F_k) must satisfy (9).

Linearization: Having obtained the discrete-time model of the system, we next compute a *variation-based* linearization of the nonlinear discrete-time dynamics around a reference trajectory as proposed in [22]. The resulting linearized model will be locally valid on the $SE(3)$ manifold, and will be used to formulate our MPC problem as a quadratic program (QP) that can be solved in real-time. To compute the linearization, we take *infinitesimal variations* with respect to a reference.

Since the position and velocity dynamics in (10) and (11) are already linear, we turn to the linearization of the orientation dynamics (12) and (13). The variations on $SO(3)$ with respect to a reference trajectory $R_k^d \in SO(3)$ is given by,

$$\delta R_k = R_k^d \hat{\eta}_k, \quad (14)$$

where $\eta_k \in \mathbb{R}^3$ and $\hat{\eta}_k$ maps $\mathbb{R}^3 \rightarrow \mathfrak{so}(3)$ such that $\hat{a}b = a \times b$ for all $a, b \in \mathbb{R}^3$, where \times is the vector cross product. The variation in the angular velocity is

$$\delta \omega_k = \frac{1}{\Delta t} (\Delta R_k \eta_{k+1} - \eta_k). \quad (15)$$

Using the variations in (14), and from the nonlinear discrete-time dynamics of the rotation matrix in (12), we get the linear discrete-time system around a reference trajectory as,

$$R_{k+1} = R_k \exp(\hat{\omega}_k \Delta t), \quad (16)$$

$$\delta R_{k+1} = \delta R_k \exp(\hat{\omega}_k^d \Delta t) + R_k^d \delta \exp(\hat{\omega}_k \Delta t), \quad (17)$$

$$\Rightarrow \eta_{k+1} = \Delta R_k^{dT} \eta_k + \Delta t \Delta R_k^{dT} \delta \omega_k. \quad (18)$$

Similarly, the linear discrete-time dynamics for the angular velocity can be obtained from (13), (14) and (15) as,

$$\delta(I \omega_{k+1}) = \delta(\Delta R_k^T I \omega_k + \Delta t \tau), \quad (19)$$

$$I \delta \omega_{k+1} = \delta \Delta R_k^T I \omega_k^d + \Delta R_k^{dT} I \delta \omega_k + \Delta t \delta \tau_{k+1}, \quad (20)$$

$$\Rightarrow I \delta \omega_{k+1} = \Delta R_k^{dT} \left(\Delta t \widehat{I \omega_k^d} + I \right) \delta \omega_k + \Delta t \delta \tau_k. \quad (21)$$

Putting together the linear and angular components, the linear discrete-time system is given by,

$$\delta \xi_{k+1} = A_k \delta \xi_k + B_k \delta F_k, \quad (22)$$

where $\delta\xi_k$ is the error state of the linearized system,

$$\delta\xi_k := [\delta p_k, \delta \dot{p}_k, \eta_k, \delta\omega_k]^T, \quad (23)$$

and A_k and B_k are given by,

$$A_k := \begin{bmatrix} \mathbb{I}_3 & \Delta t \mathbb{I}_3 & \mathbf{0}_3 & \mathbf{0}_3 \\ \mathbf{0}_3 & \mathbb{I}_3 & \mathbf{0}_3 & \mathbf{0}_3 \\ \mathbf{0}_3 & \mathbf{0}_3 & \Delta R_k^{dT} & \Delta t \Delta R_k^{dT} \\ \mathbf{0}_3 & \mathbf{0}_3 & \mathbf{0}_3 & a_\omega \end{bmatrix}, \quad (24)$$

$$B_k := \begin{bmatrix} \mathbf{0}_3 & \mathbf{0}_3 \\ \frac{\Delta t \mathbb{I}}{m} & \mathbf{0}_3 \\ \mathbf{0}_3 & \mathbf{0}_3 \\ \mathbf{0}_3 & \Delta t I^{-1} \end{bmatrix}, \quad (25)$$

$$a_\omega := I^{-1} \Delta R_k^{dT} \left(\Delta t \widehat{I\omega_k^d} + I \right). \quad (26)$$

The linear discrete-time dynamics in (22) represents the evolution of the infinitesimal variations on the manifold around a reference trajectory. These variations represent the distance between two points on the manifold. A practical and intuitive way to think about these variations is that they represent the *geometric error* between the actual state and a reference state on the manifold, under the assumption that the actual rotation matrix R_k is close to the desired rotation matrix R_k^d . If this assumption holds, then the variation $\delta\xi_k$ can be approximated as

$$\delta\xi_k \approx \begin{bmatrix} p_k - p_k^d \\ \dot{p}_k - \dot{p}_k^d \\ \frac{1}{2} \left(R_k^{dT} R_k - R_k^T R_k^d \right)^\vee \\ \omega_k - R_k^T R_k^d \omega_k^d \end{bmatrix}, \quad (27)$$

where the vee map $\vee : \mathfrak{so}(3) \rightarrow \mathbb{R}^3$ is the inverse of the hat operator, so that $\hat{x}^\vee = x \forall x \in \mathbb{R}^3$. The last two terms in (27) denote the errors on the tangent bundle $T\mathfrak{SO}(3)$ manifold [25], [26]. With this approximation, the dynamics in (22) represents the evolution of the error on the manifold locally around the reference trajectory ξ^d .

Geometric MPC-QP: Given the desired CoM states ξ_d generated from the motion library at the current trotting step, we compute the initial error state $\delta\xi(0)$ as in (27) and solve the following QP,

$$\lambda_c^* = \arg \min_{\lambda_c, \delta\xi_k, \delta F_k} \|\delta\xi_N\|_P^2 + \sum_{k=0}^N (\|\delta\xi_k\|_Q^2 + \|\delta F_k\|_R^2)$$

$$\text{s.t.} \quad \delta\xi_{k+1} = A_k(\xi_k^d) \delta\xi_k + B_k(\xi_k^d) \delta F_k, \quad (28)$$

$$\lambda_c \in \mathcal{K}_{\text{fric}}, \quad (29)$$

$$0 \leq \lambda_{c_i}^z \leq c_i \bar{\lambda}, \quad i \in \{0, 1, 2, 3\} \quad (30)$$

$$G_c \lambda_c = \delta F_0 + \begin{bmatrix} m\mathbf{g} \\ \mathbf{0}_{3 \times 1} \end{bmatrix}, \quad (31)$$

$$\delta\xi_0 = \delta\xi(0), \quad (32)$$

where (29) denotes the linearized friction-cone constraint, (32) denotes the CoM wrench and contact forces, with G_c denoting the grasp-map [27]. The constraint in (30) represents the unilateral constraints on the vertical ground reaction forces at the feet; c_i denotes the binary contact state of foot i . The QP outputs the desired contact forces for all

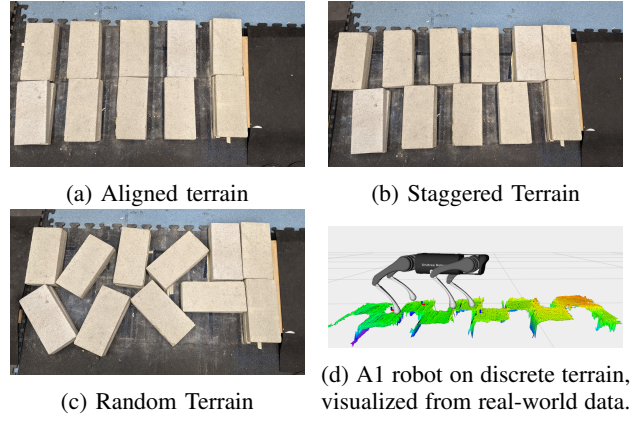


Fig. 3: Different terrains tested in our experiments, and visualization of a local map built on the robot.

legs. For legs in swing, the contact forces are set to zero by the constraint in (30). We implement the above QP using the OSQP solver [28], with a horizon length of 10 and time-step of 0.05s, which can be solved at $1e^{-4}s$. The stance-leg torques τ_{st} are then obtained through the quasi-static relation $\tau_{st} = -J_c^T \lambda_c^*$.

D. Swing leg control

For the swing-leg control, we implement an impedance controller to follow a desired foot trajectory,

$$\tau_{sw} = J_{sw}^T (-K_p^{sw} (p^{sw} - p_d^{sw}) - K_d^{sw} (\dot{p}^{sw} - \dot{p}_d^{sw})). \quad (33)$$

The desired foot trajectories are parametrized by Bézier polynomials such that the initial position is located at the true foot position at the start of a swing phase, and the desired final position based on the desired step-length, obtained through a foot-step planner (Section III-B).

E. Localization and Mapping

We use the forward facing depth camera of the A1 robot to perceive the terrain and navigate it, which makes it challenging to pick feasible footsteps for hind limbs. This requires building a local map of the robot by fusing a history of depth images that the robot sees as well as the estimate of its own inertial pose in order to build a local map of the terrain around the robot. We fuse two libraries to achieve this:

Localization: We implement contact-aided invariant EKF from [29] to localize the quadrupedal A1 robot in the world. The binary contact information, required by the EKF, is obtained through contact force sensors located at the feet.

Mapping: We utilize the probabilistic robot-centric mapping framework developed in [18], [17] to obtain a local height-map of the terrain around the robot. Localization estimates from the EKF and depth images from the robot camera are fused by the mapper to build a local map around the robot. We distinguish between steppable and un-steppable terrain based on the height and normal direction and add a 5cm threshold at the edges between these regions to account for inaccuracies in the foot placement controller and state

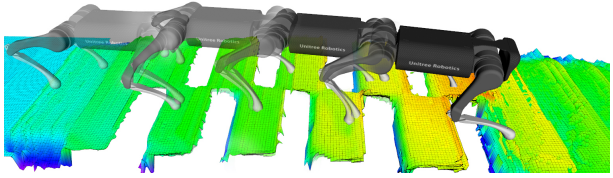


Fig. 4: Snapshots of the robot and visualization of the terrain map from real world data using our proposed approach.

estimation. The local map based on previously observed depth images is used for picking footholds for the hind limbs, eliminating the issue of lack of perception towards the back of the robot. In the future, this localization and mapping framework can be replaced by learning-based approaches, which can automatically build a history of feasible footholds.

IV. EXPERIMENTS

We demonstrate the robustness of our approach on the Unitree A1 quadruped (Fig. 3d) on a diverse set of terrains with discrete footholds (Fig. 3). These terrains consist of concrete blocks of size $6'' \times 16''$ in different positions and orientations. The gap lengths between blocks range between $7cm$ and $18cm$, and can be in different orientations. The robot is required to move in forward while avoiding the gaps. The gaps are the same for the left and right legs in the *aligned* terrain (Fig 3a), different in *staggered* (Fig. 3b) or random in *random* terrain (Fig. 3c). Random terrains pose additional constraints on the lateral foot placement. The nominal commanded velocity is $0.25m/s$ and this is updated by the gait library based on the desired foot position.

First, we compare our approach to the approach from the baseline in [13] (*Heuristic*) which uses the closest stepping location to a Raibert-like footstep and a Jacobian linearized rigid-body model, without any motion libraries. This baseline tests the robustness of our approach over other heuristic approaches from literature shown on discrete terrain walking. Next, we add motion libraries to the stance controller from [4] which uses Jacobian linearization of the CoM dynamics (*Jacobian with Gait Library*) and query CoM velocity and footstep location from the motion library. This experiment illustrates the need for geometric MPC on uneven terrain. Together, these experiments study the performance of our whole framework, against heuristic approaches from literature, as well as the importance of geometric MPC on uneven terrain. Table I summarizes the success rates of the three controllers on different terrains, over 3 hardware runs on the A1 robot. All controllers use the same vision feedback as our approach.

We conduct 3 hardware runs for each approach on the aligned and staggered terrains. We observe that the Heuristic approach is not able to successfully navigate any of the

	Heuristic	Jacobian with Gait library	GVMPC (ours)
Aligned	0/3	1/3	3/3
Staggered	0/3	0/3	2/3

TABLE I: Experiments over 3 hardware runs on the A1 robot.

terrains. This is because the robot needs to speed up when stepping over gaps due to the large size of our gaps. Since the Heuristic baseline only changes the footstep position but maintains a constant CoM height, it easily destabilized when walking over large gaps. The second baseline which uses the gait library is able to cross the aligned terrain in 1 trial, but fails on the staggered terrain. The Jacobian linearized model does not regulate the CoM velocities and orientations well in our experiments, causing the robot to go unstable. The instability is caused more in the lateral direction pointing towards foot placement feedback going unstable due to lateral and roll angular velocities. The failure mode in the staggered experiment for the GVMPC is due to the stance foot slipping at the edge of the terrain.

Additionally, we conduct two runs of experiments on the random terrain, which is significantly more complicated and needs precise foot placement, and CoM position and orientation planning. Our approach is able to navigate this terrain in 2/2 experiments. These experiments demonstrate that our proposed Geometric MPC is able to robustly stabilize the robot from a larger set of states around a desired trajectory.

V. CONCLUSIONS

In this paper, we present a planning and controls framework for vision-aided navigation for quadrupedal robots in challenging terrain. The method leverages offline computation of library of gaits parametrized by step lengths, and an on-board geometric MPC that takes into account the underlying geometric structure of the reduced-order rigid-body model, in both, the discretization and linearization of the dynamics. Combining our proposed method with existing state of the art tools for localization and mapping, we demonstrate successful implementation of locomotion on discrete terrain on a quadruped robot.

REFERENCES

- [1] Q. Nguyen, A. Agrawal, W. Martin, H. Geyer, and K. Sreenath, "Dynamic bipedal locomotion over stochastic discrete terrain," *Inter-*

- national Journal of Robotics Research (IJRR)*, pp. 1–17, August 2018.
- [2] Q. Nguyen, A. Agrawal, X. Da, W. Martin, H. Geyer, J. W. Grizzle, and K. Sreenath, “Dynamic walking on randomly-varying discrete terrain with one-step preview,” in *Robotics: Science and Systems (RSS)*, (Boston, MA), July 2017.
 - [3] A. Agrawal and K. Sreenath, “Bipedal robotic running on stochastic discrete terrain,” in *European Control Conference (ECC)*, (Naples, Italy), pp. 3564–3570, June 2019.
 - [4] J. Di Carlo, P. M. Wensing, B. Katz, G. Bledt, and S. Kim, “Dynamic locomotion in the MIT cheetah 3 through convex model-predictive control,” in *2018 IEEE/RSJ International Conference on Intelligent Robots and Systems (IROS)*, pp. 1–9, IEEE, 2018.
 - [5] S. Kajita, F. Kanehiro, K. Kaneko, K. Fujiwara, K. Harada, K. Yokoi, and H. Hirukawa, “Biped walking pattern generation by using preview control of zero-moment point,” in *2003 IEEE International Conference on Robotics and Automation (Cat. No. 03CH37422)*, vol. 2, pp. 1620–1626, IEEE, 2003.
 - [6] J. E. Pratt and R. Tedrake, “Velocity-based stability margins for fast bipedal walking,” in *Fast motions in biomechanics and robotics*, pp. 299–324, Springer, 2006.
 - [7] M. Dai, X. Xiong, and A. Ames, “Bipedal walking on constrained footholds: Momentum regulation via vertical com control,” *arXiv preprint arXiv:2104.10367*, 2021.
 - [8] Q. Nguyen, A. Hereid, J. W. Grizzle, A. D. Ames, and K. Sreenath, “3d dynamic walking on stepping stones with control barrier functions,” in *2016 IEEE 55th Conference on Decision and Control (CDC)*, pp. 827–834, IEEE, 2016.
 - [9] Q. Nguyen and K. Sreenath, “Safety-critical control for dynamical bipedal walking with precise footstep placement,” *IFAC-PapersOnLine*, vol. 48, no. 27, pp. 147–154, 2015.
 - [10] Q. Nguyen, X. Da, J. Grizzle, and K. Sreenath, “Dynamic walking on stepping stones with gait library and control barrier functions,” in *Algorithmic Foundations of Robotics XII*, pp. 384–399, Springer, 2020.
 - [11] R. Grandia, A. J. Taylor, A. D. Ames, and M. Hutter, “Multi-layered safety for legged robots via control barrier functions and model predictive control,” *arXiv preprint arXiv:2011.00032*, 2020.
 - [12] V. Tsounis, M. Alge, J. Lee, F. Farshidian, and M. Hutter, “Deepgait: Planning and control of quadrupedal gaits using deep reinforcement learning,” *IEEE Robotics and Automation Letters*, vol. 5, no. 2, pp. 3699–3706, 2020.
 - [13] Z. Xie, X. Da, B. Babich, A. Garg, and M. van de Panne, “Glide: Generalizable quadrupedal locomotion in diverse environments with a centroidal model,” *arXiv preprint arXiv:2104.09771*, 2021.
 - [14] Z. Xie, H. Y. Ling, N. H. Kim, and M. van de Panne, “Allsteps: Curriculum-driven learning of stepping stone skills,” in *Computer Graphics Forum*, vol. 39, pp. 213–224, Wiley Online Library, 2020.
 - [15] A. Siravuru, A. Wang, Q. Nguyen, and K. Sreenath, “Deep visual perception for dynamic walking on discrete terrain,” in *2017 IEEE-RAS 17th International Conference on Humanoid Robotics (Humanoids)*, pp. 418–424, IEEE, 2017.
 - [16] O. Villarreal, V. Barasuol, P. M. Wensing, D. G. Caldwell, and C. Semini, “Mpc-based controller with terrain insight for dynamic legged locomotion,” in *2020 IEEE International Conference on Robotics and Automation (ICRA)*, pp. 2436–2442, IEEE, 2020.
 - [17] P. Fankhauser, M. Bloesch, C. Gehring, M. Hutter, and R. Siegwart, “Robot-centric elevation mapping with uncertainty estimates,” in *International Conference on Climbing and Walking Robots (CLAWAR)*, 2014.
 - [18] P. Fankhauser, M. Bloesch, and M. Hutter, “Probabilistic terrain mapping for mobile robots with uncertain localization,” *IEEE Robotics and Automation Letters (RA-L)*, vol. 3, no. 4, pp. 3019–3026, 2018.
 - [19] A. Hereid, E. A. Cousineau, C. M. Hubicki, and A. D. Ames, “3d dynamic walking with underactuated humanoid robots: A direct collocation framework for optimizing hybrid zero dynamics,” in *2016 IEEE International Conference on Robotics and Automation (ICRA)*, pp. 1447–1454, IEEE, 2016.
 - [20] A. Hereid, O. Harib, R. Hartley, Y. Gong, and J. W. Grizzle, “Rapid trajectory optimization using c-frost with illustration on a cassie-series dynamic walking biped,” in *2019 IEEE/RSJ International Conference on Intelligent Robots and Systems (IROS)*, pp. 4722–4729, IEEE, 2019.
 - [21] M. Chignoli and P. M. Wensing, “Variational-based optimal control of underactuated balancing for dynamic quadrupeds,” *IEEE Access*, vol. 8, pp. 49785–49797, 2020.
 - [22] G. Wu and K. Sreenath, “Variation-based linearization of nonlinear systems evolving on $so(3)$ and s^2 ,” *IEEE Access*, vol. 3, pp. 1592–1604, September 2015.
 - [23] S. Hong, J.-H. Kim, and H.-W. Park, “Real-time constrained nonlinear model predictive control on $so(3)$ for dynamic legged locomotion,” in *2020 IEEE/RSJ International Conference on Intelligent Robots and Systems (IROS)*, pp. 3982–3989, IEEE, 2020.
 - [24] A. Siravuru, S. P. Viswanathan, K. Sreenath, and A. K. Sanyal, “The reaction mass biped: Geometric mechanics and control,” *J. Intell. Robot. Syst.*, vol. 89, no. 1–2, pp. 155–173, 2018.
 - [25] T. Lee, M. Leok, and N. H. McClamroch, “Control of complex maneuvers for a quadrotor uav using geometric methods on $se(3)$,” *arXiv preprint arXiv:1003.2005*, 2010.
 - [26] F. Bullo and A. D. Lewis, *Geometric control of mechanical systems: modeling, analysis, and design for simple mechanical control systems*, vol. 49, Springer, 2019.
 - [27] R. M. Murray, Z. Li, and S. S. Sastry, *A mathematical introduction to robotic manipulation*. CRC press, 2017.
 - [28] B. Stellato, G. Banjac, P. Goulart, A. Bemporad, and S. Boyd, “OSQP: an operator splitting solver for quadratic programs,” *Mathematical Programming Computation*, vol. 12, no. 4, pp. 637–672, 2020.
 - [29] R. Hartley, M. Ghaffari, R. M. Eustice, and J. W. Grizzle, “Contact-aided invariant extended kalman filtering for robot state estimation,” *The International Journal of Robotics Research*, vol. 39, no. 4, pp. 402–430, 2020.